



Bunch-length measurement at a bunch-by-bunch rate based on time–frequency-domain joint analysis techniques and its application

Hong-Shuang Wang^{1,2} · Xing Yang^{1,2} · Yong-Bin Leng^{1,3} · Yi-Mei Zhou⁴ · Ji-Gang Wang³

Received: 13 October 2023 / Revised: 29 November 2023 / Accepted: 21 December 2023 / Published online: 24 May 2024

© The Author(s), under exclusive licence to China Science Publishing & Media Ltd. (Science Press), Shanghai Institute of Applied Physics, the Chinese Academy of Sciences, Chinese Nuclear Society 2024

Abstract

This paper presents a new technique for measuring the bunch length of a high-energy electron beam at a bunch-by-bunch rate in storage rings. This technique uses the time–frequency-domain joint analysis of the bunch signal to obtain bunch-by-bunch and turn-by-turn longitudinal parameters, such as bunch length and synchronous phase. The bunch signal is obtained using a button electrode with a bandwidth of several gigahertz. The data acquisition device was a high-speed digital oscilloscope with a sampling rate of more than 10 GS/s, and the single-shot sampling data buffer covered thousands of turns. The bunch-length and synchronous phase information were extracted via offline calculations using Python scripts. The calibration coefficient of the system was determined using a commercial streak camera. Moreover, this technique was tested on two different storage rings and successfully captured various longitudinal transient processes during the harmonic cavity debugging process at the Shanghai Synchrotron Radiation Facility (SSRF), and longitudinal instabilities were observed during the single-bunch accumulation process at Hefei Light Source (HLS). For Gaussian-distribution bunches, the uncertainty of the bunch phase obtained using this technique was better than 0.2 ps, and the bunch-length uncertainty was better than 1 ps. The dynamic range exceeded 10 ms. This technology is a powerful and versatile beam diagnostic tool that can be conveniently deployed in high-energy electron storage rings.

Keywords Bunch-by-bunch diagnostic · Bunch-length measurement · Synchronous phase measurement · Joint time–frequency-domain analysis · Longitudinal instability

This work was supported by the National Key R&D Program (No. 2022YFA1602201).

✉ Yong-Bin Leng
lengyb@ustc.edu.cn

¹ Shanghai Institute of Applied Physics, Chinese Academy of Sciences, Shanghai 201800, China

² University of Chinese Academy of Sciences, Beijing 100049, China

³ National Synchrotron Radiation Laboratory, University of Science and Technology of China, Hefei 230026, China

⁴ Shanghai Advanced Research Institute, Chinese Academy of Sciences, Shanghai 201204, China

1 Introduction

In recent decades, advances in accelerator technology have resulted in a reduced beam size and emittance, necessitating advanced beam diagnostic techniques. The bunch length, a fundamental parameter in accelerator systems, is critical for determining brightness and emittance. Therefore, accurate bunch-length measurements are vital for ensuring stable accelerator operation.

Several methods have been developed for bunch-length measurements, including streak cameras, transverse deflecting cavities [1, 2], electro-optical sampling, autocorrelators, cross-correlators [3, 4], and spectral analyses. Streak cameras are widely used in laboratories such as NSLS-II [5], SSRF [6], PEP-II [7], ANKA [8, 9], and BESSY II [10]. Streak cameras offer precise measurements of the longitudinal bunch length and the spatial distribution of individual bunches without impacting the beam. When the dynamic

range is set sufficiently small, many details, such as the filamentation of freshly injected bunches in real space, can be observed on a picosecond scale [11]. However, the limitation of streak cameras lies in their finite pixel units determined by the measurement device (CCD). This makes it challenging to simultaneously achieve an extensive dynamic range and high time resolution.

A typical example is the measurement of the damping time of injected bunches at ALBA in 2012. They observed the process with a streak camera that was required to cover the entire injection process, resulting in a limited time resolution and an inability to resolve the evolution on a turn-by-turn basis. In 2018, the ALBA group focused on the amplitude and frequency of longitudinal oscillations, which required a streak camera with high time resolution to observe the waveform of the bunches. However, the dynamic range of the streak camera could not cover the entire damping oscillation process, making it impossible to determine the damping time accurately [12, 13].

In 2016, BINP SB RAS developed a dissector measurement technique similar to that of a streak camera [14]. The dissector converts light signals into electrical signals and uses photomultiplier tubes for measurements. Metrology Light Source (MLS) used a dissector for bunch-length measurements in combination with a streak camera [15]. However, dissectors lack universality and high resolution and cannot fully replace streak cameras.

Although electro-optical sampling is commonly used in linear accelerators, efforts have been made to apply it to storage rings. For example, the KIT storage ring KARA performed longitudinal single-shot optical detection of electron bunches and obtained valuable data for long-timescale measurements [16]. The analysis of the beam charge density cloud distribution and the dynamic properties of the beam profile followed this [17]. By leveraging electro-optical sampling, the complete spectral information of coherent synchrotron radiation was obtained [18]. However, the use of electro-optical sampling as a general diagnostic technique for storage rings has been limited.

In the bunch spectrum analysis, the dual-frequency method showed a relatively high measurement accuracy. Significant progress has been made by research institutions, such as KEKB [19, 20] and ANKA [21]. However, traditional dual-frequency systems have narrow bandwidths and can only provide the average bunch length for multiple bunches over multiple turns. In 2014, SSRF [22, 23] explored a dual-frequency-based bunch-by-bunch bunch-length measurement technique. However, owing to the limited signal-to-noise ratio and significant inter-bunch crosstalk, the measurement accuracy did not meet the requirements of most machine studies. In another development, PLS-II [24] used fast photodiodes to detect synchronous light signals and analyzed

the spectral structure to calculate the bunch length. However, limitations in signal processing prevented bunch-by-bunch and turn-by-turn measurements, and the probe bandwidth was insufficient to measure sub-20-ps bunches accurately.

Since 2012, the SSRF beam instrumentation group has developed a multiparameter diagnostic method for electron storage rings based on broadband random sampling technology. This method uses button-electrode signals and visible synchronized radiation as sources, high-speed digital oscilloscopes as data acquisition devices, and offline software to analyze the data collected by the oscilloscopes. It accurately measured parameters such as charge, transverse position [25, 26], bunch length, longitudinal phase [27], and transverse bunch size [28]. On this basis, an open-source software package called HOTCAP [29] was developed to complete the measurement of three-dimensional position and charge simultaneously [30], which can be applied to any high-energy electron storage ring. Numerous application studies have been conducted based on this tool, including the evaluation of injection dynamics [31], analysis of transverse wakefields [32], observation of longitudinal damping oscillations of refilled bunches [33], in situ diagnosis of optical parameters [34], and assessment of beam-loading effects in harmonic cavities.

The remainder of this paper is divided as follows: Sect. 2, basic principles and fundamentals related to bunch-length calculation. Section 3, the experimental setup, including the platform, measurement system, bunch-length calculation process, and uncertainty evaluation. Section 4, the beam experiment and results, including separate results from HLS and SSRF. Section 5, a discussion of the results, and Sect. 6, the conclusion.

2 Theoretical basis

2.1 Determinants of bunch length

The bunch length in a storage ring can be determined using electron-optical machine parameters. If the beam energy spread follows a Gaussian distribution, the root-mean-square (RMS) bunch length can be given by

$$\sigma_{\Delta_s} = \frac{c\eta_c}{\Omega} \frac{\sigma_p}{p_0} = \sqrt{\frac{c^3}{2\pi q} \frac{p_0 \beta_0 \eta_c}{hf_0^2 V \cos(\phi_s)} \frac{\sigma_p}{p_0}}, \quad (1)$$

where $\frac{\sigma_p}{p_0}$ is the relative momentum spread of the beam, p_0 is the equilibrium particle momentum, η_c is the momentum compaction factor, f_0 is the particle revolution frequency, V is the equivalent longitudinal electrical field (RF field, harmonic cavity field, and wakefield), and ϕ_s is the synchronous phase. The longitudinal distribution of the bunch is determined using the equivalent longitudinal electrical field, energy spread, acceleration phase, and

momentum compaction factor. The bunch length is a crucial beam parameter that reflects whether the electron storage ring meets the design specifications or is in a good operational condition. Accurate measurement of the bunch length is essential for stable operation of the accelerator and acceptance testing of newly constructed facilities.

In the storage ring, variations in the bunch length arise primarily from changes in the effective longitudinal electrical field, V , and acceleration phase, ϕ_s . For example, longitudinal dipole oscillations can occur when longitudinal instabilities occur, resulting in changes in ϕ_s . When fresh bunches are injected, the initial phase of the injected bunches deviates from the equilibrium. Changes in V and ϕ_s can occur because of tuning of the RF system or transient effects from the beam wakefields. Precise quantitative analysis of these phenomena can be achieved by capturing and measuring the bunch-length evolution on a turn-by-turn basis. This provides a powerful tool for nonlinear beam dynamics research. Therefore, the accurate diagnosis and measurement of the bunch length on a bunch-by-bunch and turn-by-turn basis are crucial for storage rings.

Assuming that the bunch length is only related to V and ϕ_s , Eq. (1) can be written as

$$\sigma_{\Delta_s}(V, \phi_s) = a / \sqrt{V \cos(\phi_s)}, \tag{2}$$

where $a = \sqrt{\frac{c^3}{2\pi q} \frac{\rho_0 \beta_0 \eta_c}{hf_0^2} \frac{\sigma_p}{\rho_0}}$ denotes a constant for each machine. Taking the partial derivatives of Eq. (2), we obtain:

$$\frac{\partial \sigma_{\Delta_s}(V, \phi_s)}{\partial V} = -\frac{\sigma_{\Delta_s}}{2V}, \tag{3}$$

$$\frac{\partial \sigma_{\Delta_s}(V, \phi_s)}{\partial \phi_s} = \frac{\sigma_{\Delta_s}}{2 \cot(\phi_s)}. \tag{4}$$

Thus, when the RF cavity voltage and bunch phase change within a small range, the change in bunch length $\Delta\sigma$ is linearly related to the change in the cavity voltage ΔV and phase $\Delta\phi_s$.

2.2 Bunch-length measurement principle

For an ideal Gaussian distribution, the beam signal in the time domain is given by

$$I(t) = \frac{Q}{\sqrt{2\pi}\sigma} \exp\left[-\frac{(t-t_0)^2}{2\sigma^2}\right], \tag{5}$$

where Q denotes the bunch charge, σ is the bunch length, and t_0 is the bunch phase. The principle of beam signal acquisition in a storage ring is illustrated in Fig. 1a and b.

When the beam passes through the button electrode, the detected signal can be expressed as follows:

$$V_b(t) = \frac{\pi a^2}{2\pi b} \frac{1}{\beta c} Z \frac{t-t_0}{\sigma^2} I(t) F(\delta, \theta). \tag{6}$$

In Eq. (6), a and b represent the physical dimensions of the button electrode, $F(\delta, \theta)$ represents the transverse position of the bunch, and Z represents the transfer impedance of the button electrode. The beam distribution and the detected signal are shown in Fig. 1c, with the characteristics of a Gaussian distribution and bipolar pulse, respectively.

In the time domain, the detected signal (voltage signal) can be expressed as the convolution of the beam signal (current signal) and the detection system impulse response:

$$V_b(t) = I(t) * H_{\text{Button}}, \tag{7}$$

where H_{Button} is the time-domain response function. In the frequency domain, we have

$$V(f) = I(f) \cdot R_{\text{Button}}(f) = Q \cdot \exp\left(-\frac{\omega^2}{2\sigma_f^2}\right) \cdot R_{\text{Button}}(f), \tag{8}$$

where $V(f)$ is the frequency-domain distribution of the detected signal, $I(f)$ is the frequency-domain distribution of the beam signal (Gaussian distribution), $R_{\text{Button}}(f)$ is the frequency-domain transfer impedance, and σ_f is the reciprocal of the time-domain bunch length. Therefore, by measuring σ_f , the bunch length can be determined.

3 Experimental measurement system setup

3.1 Experimental platform

Beam experiments were conducted at HLS and SSRF. The key parameters of the two facilities are listed in Table 1.

3.2 Measurement system structure

The structure of the bunch-by-bunch measurement system is illustrated in Fig. 2. First, four-electrode signals from the BPM probes were acquired using a high sampling rate and high-bandwidth digital oscilloscope. The signals were imported into a Python script for further analysis. In the three-dimensional bunch position calculation module of the script, the four-channel data were concatenated to form a bunch-by-bunch beam signal. The response function was reconstructed, and the longitudinal center position (phase) information of the bunch was extracted in the time domain using the response function vector projection method. The reconstructed response function was resampled to obtain the

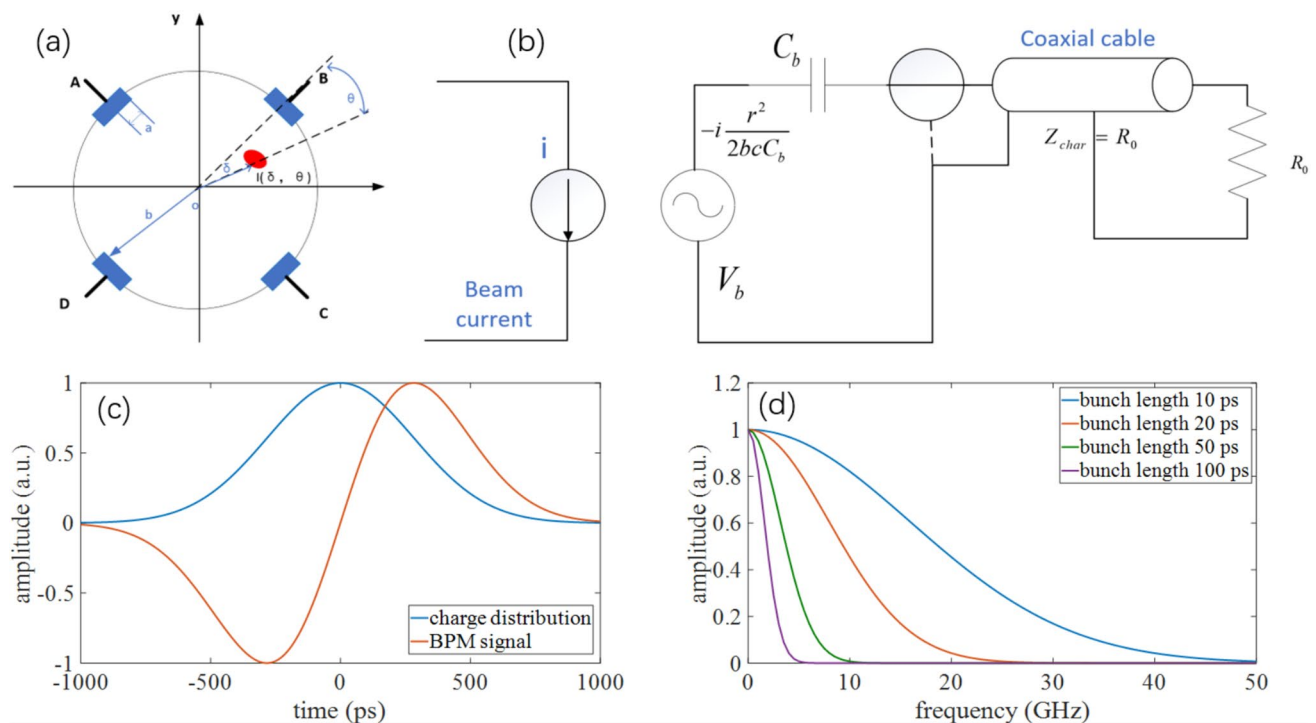


Fig. 1 (Color online) **a** Transverse cross-section of the storage ring beam pipe with four-channel button electrode. **b** Equivalent circuit for signal pickup in a BPM. **c** Ideal longitudinal beam charge distribu-

tion and waveform of the BPM acquisition signal. **d** Ideal frequency-domain distribution of the BPM signal for bunch lengths ranging from 10 to 100 ps

Table 1 Machine parameters

Parameter	SSRF	HLS
Energy, E (GeV)	3.5	0.8
Current, I_0 (mA)	200	400
Main RF cavity	SC	Copper
Harmonic cavity	3rd SC	4rd copper
RF frequency, f_{rf} (MHz)	499.654	204.03
Buckets, h	720	45
Designed bunch length, σ (ps)	18	50

signal amplitude for each bunch. The transverse position and charge information of the bunch were obtained by applying the difference and ratio algorithms.

3.3 Bunch-length calculation process

The bunch-length calculation module calibrates the transfer impedance of the measurement system. Figure 3a–e shows the calibration process. The original continuous sampling data were sliced bunch-by-bunch and turn-by-turn. Single-bunch single-turn data were subjected to spectral analysis after baseline subtraction. A streak camera was used to measure the bunch length and calculate the expected signal spectrum distribution. The measured signal spectrum

(voltage spectrum) was divided by the expected signal spectrum (current spectrum) to obtain the system transfer function (impedance). Assuming that the machine parameters of the storage ring remain constant, the system transfer impedance is a known quantity and does not require recalibration during subsequent data acquisition and processing. For the bunch-length calculation, all measurement data were sliced and harmonically analyzed, and the background was subtracted to obtain the voltage signal spectrum. Dividing the voltage signal spectrum by the system transfer function yields the current signal spectrum. Gaussian fitting was performed on this spectrum to determine the bunch-length measurement results for each bunch and turn. Figure 3f–i demonstrates the data processing with different charges of 0.18 nC, 1.16 nC, and 2.39 nC, showing distinct differences in spectrum distribution. Gaussian fitting of the spectra enables the determination of the bunch lengths as 65 ps, 83 ps, and 88 ps, respectively.

3.4 Uncertainty evaluation

At HLS, where significant longitudinal instability occurs, the uncertainty of the bunch-length measurement system was evaluated in the single-bunch mode. By progressively increasing the charge of a single bunch and using principal component analysis (PCA) to separate

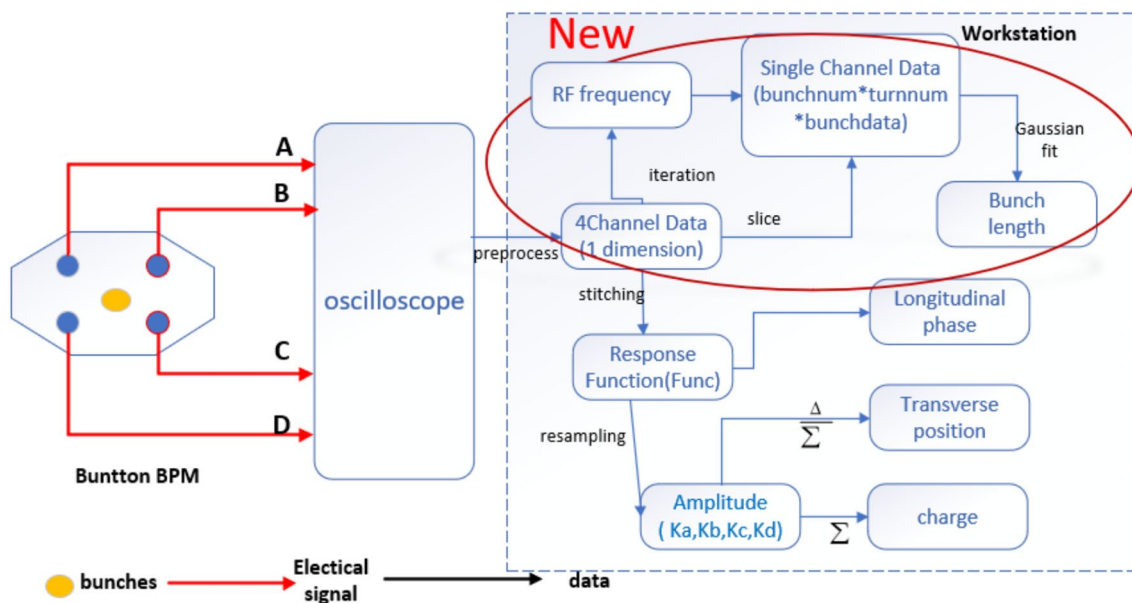


Fig. 2 Overall schematic of the bunch-by-bunch measurement system in the storage ring

the bunch oscillation modes during longitudinal instability, the residual measurement data were calculated as the measurement uncertainty of the system (Fig. 4a). In SSRF, where there is no apparent longitudinal instability in the normal operation mode, the random errors of the measurement system were evaluated in the multibunch operation mode. Assuming a constant bunch length for each bunch, the standard deviation of the bunch-length measurement for multiple turns of each bunch was calculated as the measurement uncertainty of the system. The dependence of the bunch-length measurement uncertainty on the bunch charges was analyzed for 500 bunches (Fig. 4b). Both experiments show that the bunch-length measurement uncertainty is inversely proportional to the bunch charge, aligning with expectations.

4 Beam experiment and results

To validate the performance of the new system, we measured the bunch length under different charge conditions for a single bunch at HLS. We also observed a longitudinal instability in the normal operating state of the storage ring. We also measured the dependence of the bunch length on the bunch charge at SSRF. We investigated the variations in bunch length with the total beam current during the harmonic cavity tuning process. In addition, we captured and analyzed random events related to coherent beam instability.

4.1 Experiment at HLS

In the single-bunch experiment at HLS, the bunch charge varied from 0.2 nC to 2.6 nC. The bunch length was synchronously measured using a streak camera and high-speed oscilloscope in the time–frequency analysis system. The average bunch lengths obtained using both methods are in excellent agreement, as shown in Fig. 5a. Bunch-length variation with different bunch currents is because of the longitudinal broad impedance, formulated by [35]

$$\left(\frac{\sigma_t}{\sigma_{t0}}\right)^3 - \frac{\sigma_t}{\sigma_{t0}} = \frac{I_b \alpha}{\sqrt{2\pi} v_s^2 \omega_0^3 \sigma_{t0}^3 E/e} \text{Im}\left(\frac{Z_{||}}{n}\right)_{\text{eff}}, \tag{9}$$

where α is the momentum compaction factor, $v_s = \omega_s/\omega_0$ is the synchrotron tune, and σ_{t0} is the bunch length at zero intensity. We calculated the longitudinal broadband impedance of HLS to be 7.1 Ω .

In addition to providing the average bunch length, the time–frequency analysis system captured the evolution of the bunch length on a turn-by-turn basis. As shown in Fig. 5b, the bunch length remained constant when the bunch charge was relatively low (0.18 nC). However, significant longitudinal instability occurred for bunch charges above a certain threshold, resulting in periodic oscillations in the bunch length. A harmonic analysis of the turn-by-turn bunch-length variations (Fig. 5c) revealed that the oscillation frequency decreased as the bunch charge increased. Similarly, the harmonic analysis of the

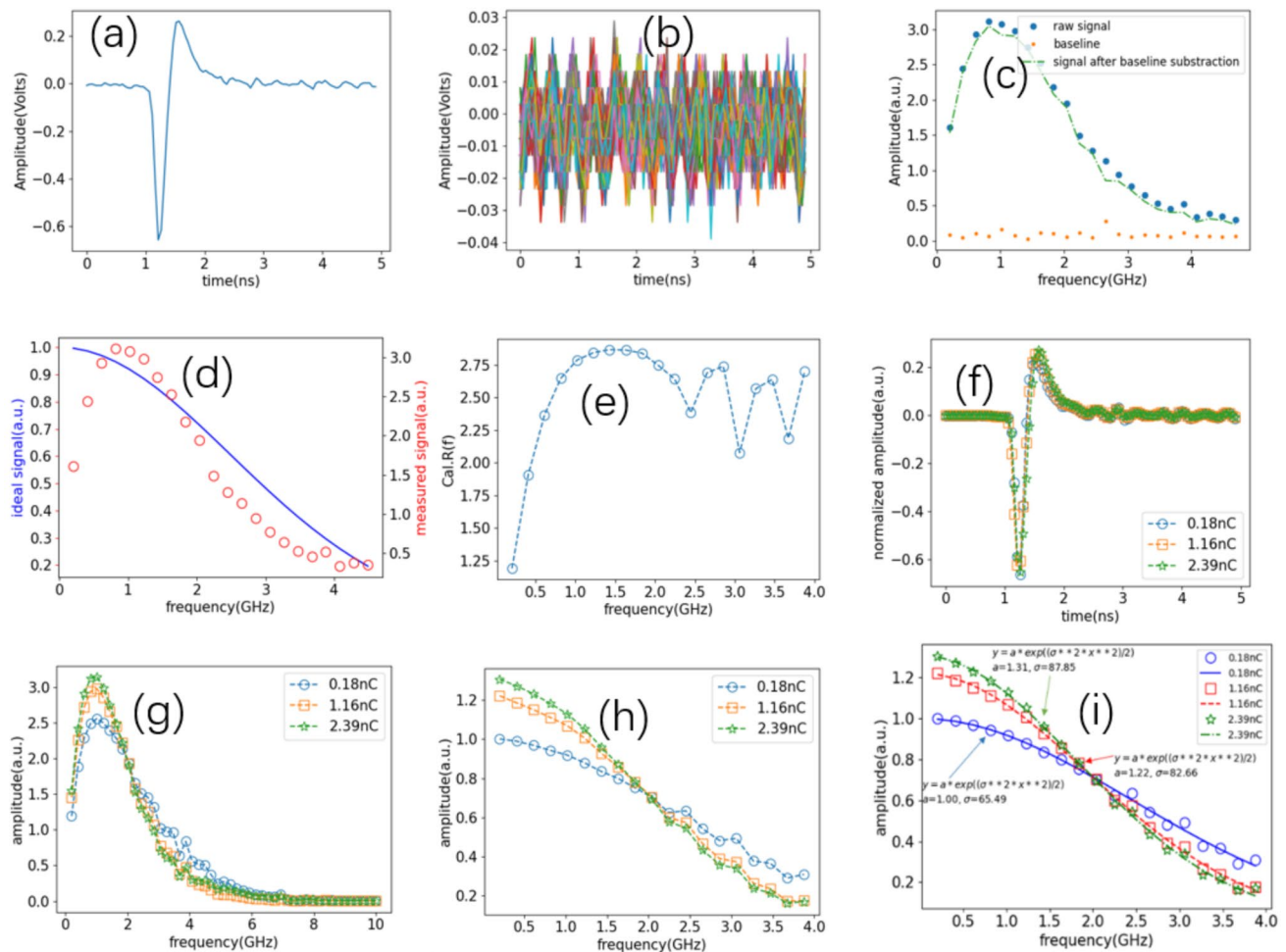
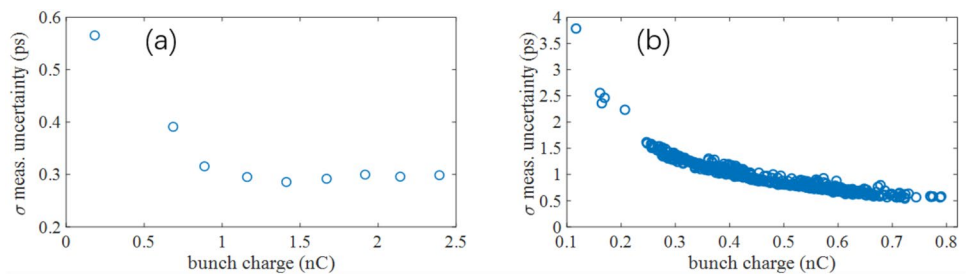


Fig. 3 (Color online) **a** Waveform of the raw signal from a single bunch in one turn. **b** Background noise in the absence of beam bunches. **c** Spectrum of the original signal, background noise, and the signal with the background noise removed. **d** Comparison of the frequency-domain distribution between the ideal signal and the measured data. **e** Frequency-domain transfer impedance calibrated using a

streak camera. **f** Waveform of the raw signal from a single bunch with charges of 0.18 nC, 1.16 nC, and 2.39 nC. **g** Frequency-domain waveform with three different charges. **h** Frequency-domain distributions after calibration with three different charges. **i** Gaussian fitting on the three bunches with different charges, yielding their respective beam lengths ranging from 65 ps to 88 ps

Fig. 4 (Color online) **a** Uncertainty assessment of bunch-length measurements for different charges in the single-bunch mode at HLS. **b** Multibunch operation mode at SSRF, the charge, and bunch-length uncertainty for each individual bunch



turn-by-turn phase variations (Fig. 5d) shows oscillation modes in complete synchronization with bunch-length oscillations.

Owing to the use of a room temperature copper cavity as the main RF cavity at HLS, the higher-order mode (HOM) issues are quite severe. Additionally, there are numerous

discontinuous beamline components in the storage ring, such as stripline beam position monitors (SBPM), beam scrubbing electrodes, and vacuum insertions, which result in a relatively high impedance and make the occurrence of longitudinal instabilities more likely. To investigate this, a typical dataset was recorded using the measurement system

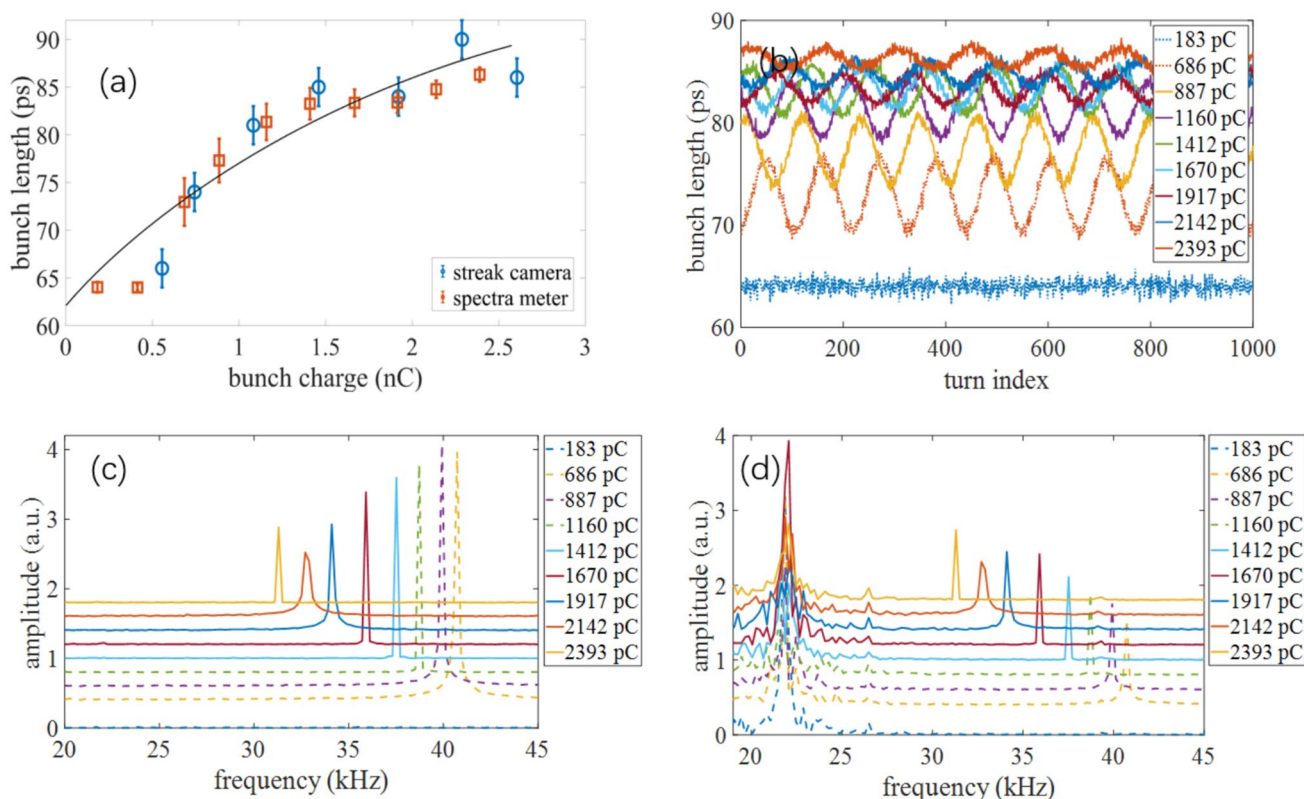


Fig. 5 (Color online) **a** HLS single-bunch experiment bunch-length distribution with respect to bunch charge. Time–frequency analysis system results show excellent agreement with streak camera results. **b** Under different charges, the bunch length exhibits noticeable oscillations when the charge exceeds a certain threshold. **c** The spectrum

of bunch-length oscillations varies with different charges; the peak of the spectrum shifts to the left as the charge increases. **d** The spectrum of phase oscillations varies with different charges, exhibiting the same oscillation mode as the bunch length and a common oscillation peak

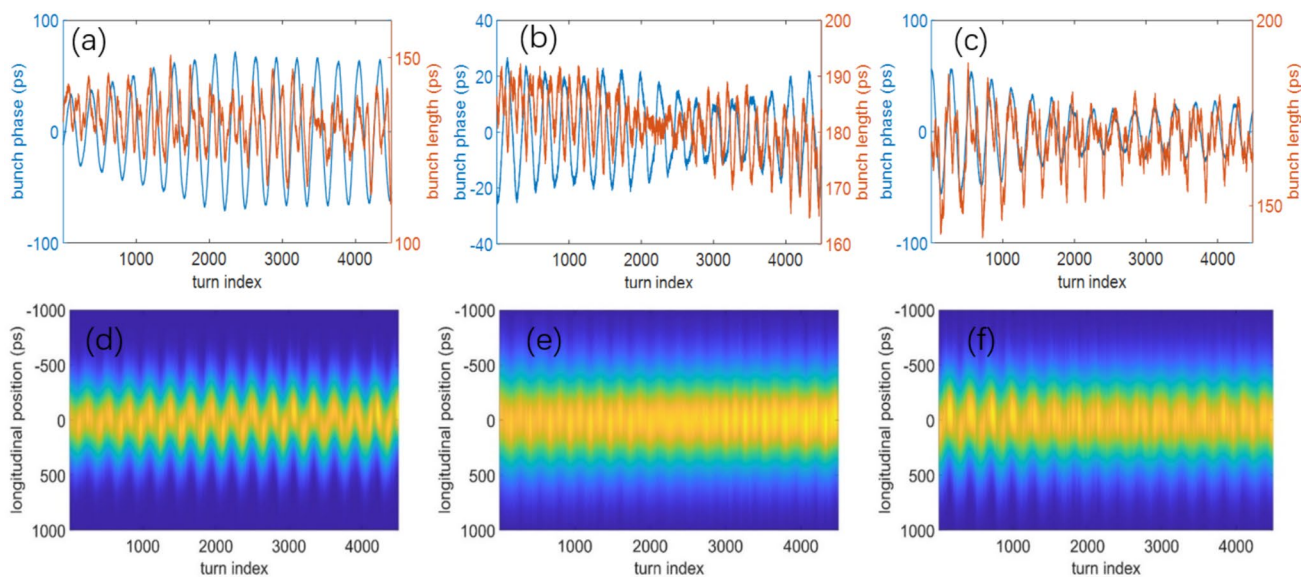


Fig. 6 (Color online) **a–c** Oscillations of the longitudinal center position (phase) and bunch length for the head, middle, and tail bunches, respectively. **d–f** Reconstructed longitudinal distributions (including phase and bunch length) for the head, middle, and tail bunches, respectively

in normal operation mode at HLS (total current of 400 mA with 35 continuously filled bunches). Figure 6a–c shows the longitudinal center position and bunch length of the head, middle, and tail bunches, respectively, as a function of time. Figure 6d–f presents the corresponding reconstructed distributions. It is evident that both oscillations in the bunch center positions and bunch lengths are significant, and their frequencies are in agreement, as expected. Additionally, the amplitudes of the oscillations were larger at the head and tail of the bunch train than in the middle (Fig. 6).

4.2 Experiment at SSRF

At SSRF, the charge of a single bunch was gradually increased from 2 to 9.5 nC. The variation in the bunch length with respect to the bunch charge was measured using the time–frequency analysis system with an oscilloscope, as shown in Fig. 7a. The bunch length exhibited localized nearly linear increases with the bunch charge. We also calculated the longitudinal broadband impedance as 0.3Ω , which is in good agreement with the design value [36].

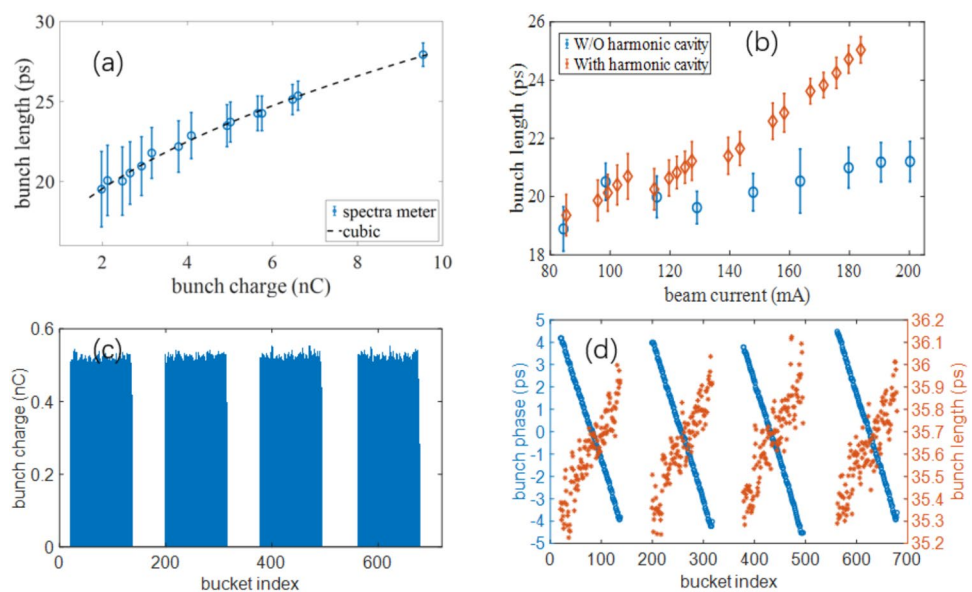
During harmonic cavity tuning, we measured the average bunch length as a function of the total beam current. The measurements were conducted in top-up mode with regularly spaced four-bunch trains, each containing 125 bunches. The total beam current varied from 80 mA to 180 mA. The results are shown in Fig. 7b (marked by red diamonds), with a comparison provided for the case of the harmonic cavity set to the non-working state, showing the variation in the average bunch length with the beam current (marked by blue circles). By comparing the measurement results, it is evident that the harmonic cavity exhibited a stretching effect on the bunches. However, the stretching factor was

significantly smaller than the design target, indicating room for optimization.

This process was continued by decreasing the detuning frequency of the harmonic cavity and increasing the total beam current to 200 mA (Fig. 7c), owing to beam-loading effects, there were variations in both the bunch phase and bunch length at different positions within the bunch train. The results are presented in Fig. 7d and are consistent with the simulation results of CEPC [37]. The difference in bunch length between the head and tail of the bunch train, which was less than 1 ps, was distinguishable. Additionally, a negative correlation was observed between the bunch length and phase within the bunch train. Assuming an uncertainty of 1 ps for the turn-by-turn measurements, the random error after averaging 7000 turns was determined to be less than 0.02 ps, which agreed with the measurement results.

During the process of optimizing the harmonic cavity, when there was a mismatch between the main RF cavity and the harmonic cavity, the stored bunches deviated significantly from their equilibrium positions owing to large longitudinal kick forces. This resulted in coherent longitudinal dipole oscillations with a substantial amplitude occurring at a frequency close to the stabilized working frequency (normalized frequency of 0.005) of the main RF system after closed-loop operation. When such instability occurs, the beam signal amplitude exceeds the normal operating state owing to coupling between the longitudinal and transverse motions. These random events can be captured by setting the appropriate signal trigger thresholds. To reduce random measurement errors, we averaged the phase and bunch-length data for all 500 bunches, as shown in Fig. 8a. Analysis of the time–frequency-domain characteristics of the oscillation waveform revealed that the frequency of the longitudinal phase oscillation and

Fig. 7 (Color online) **a** SSRF single-bunch experiment relationship between beam length and uncertainty with respect to the beam charge. **b** Comparison of beam-length measurement results with and without harmonic cavity during the beam accumulation process in the multibunch at SSRF. **c** Injection mode for the multibunch at SSRF. **d** Distribution of the phase and beam length within each individual bunch in the bunch train



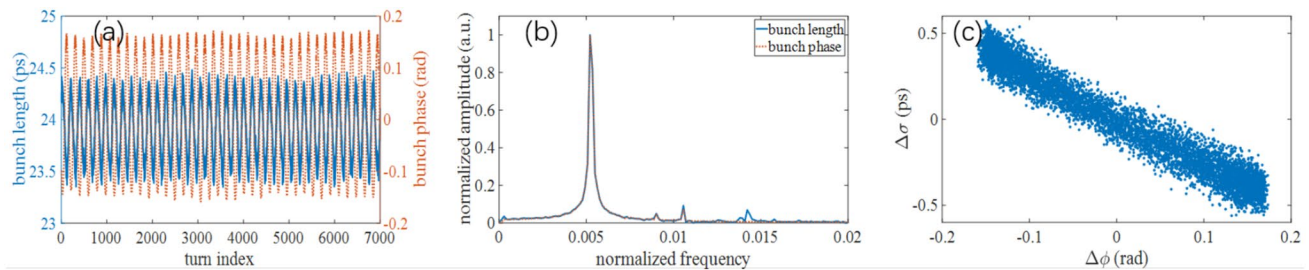


Fig. 8 (Color online) **a** Oscillations of beam length and phase when longitudinal instability occurs. **b** Spectrum of the beam length and phase oscillations when longitudinal instability occurs, with both

normalized oscillation frequencies at approximately 0.005. **c** Negative correlation between the change in beam length and the change in phase

the bunch-length oscillation completely matched, but the oscillation phase was the opposite. The random error in the turn-by-turn bunch-length measurements, obtained through multibunch averaging, could be reduced to less than 0.05 ps, and the sinusoidal bunch-length oscillation waveform with a peak-to-peak amplitude of approximately 1.5 ps could be perfectly reproduced. Analyzing the changes in the bunch length and phase during the occurrence of instability, a strong negative linear relationship between the two was observed, which is consistent with the previous theoretical analyses.

5 Discussion

For most electron storage rings serving synchrotron light sources or colliders, the bunch length typically ranges from tens to hundreds of picoseconds. Based on the simulation analysis and experimental results of this study, data acquisition systems with several gigahertz analog bandwidths and tens of gigahertz sampling rates can fully meet the requirements for bunch-length measurement resolution. The developed bunch-length measurement system can be conveniently deployed and applied to any electron storage ring based on commercial digital oscilloscopes and utilizing time–frequency-domain joint analysis.

With a Gaussian longitudinal distribution and bunch length ranging from 20 to 200 ps, the measurement uncertainty of the bunch length on a turn-by-turn basis can be better than 1 ps for bunch charges greater than 400 pC. The measurement dynamic range can exceed 10 ms. However, the single-bunch and single-turn bunch-length resolutions have not yet reached a level that can be directly applied to all high-resolution beam experiments. However, when focusing on the average bunch length among different bunches (such as the distribution of the bunch length within a bunch train during steady-state operation), the turn-by-turn measurement results for each bunch can be averaged to reduce the random measurement error to less than 0.02

ps. When the focus is on the common-mode variations of all bunches in the storage ring (such as the occurrence of coherent longitudinal oscillations), the measurement results for the same turn of multiple bunches can be averaged to reduce the random measurement error to less than 0.05 ps.

The current time–frequency-domain joint analysis bunch-length measurement technique assumes a Gaussian distribution for the bunch, providing only the σ parameter as a characteristic quantity for the measurement result. Therefore, it cannot fully replace streak cameras. When the longitudinal bunch distribution deviates from a standard Gaussian distribution (such as filamentation during the damping process after injection or significant wakefield effects resulting in an off-centered Gaussian distribution), the results are approximate. Further improvements to the system sampling rate and obtaining more accurate measurements of the beam signal spectrum coupled with appropriate data fitting models, may enable more characteristic parameters to be used as measurement results, and even obtain the original time-domain distribution through inverse Fourier transformation.

6 Conclusion

This study presents a novel technique for measuring the bunch length on a bunch-by-bunch basis, utilizing time–frequency analysis of the beam signal acquired by an oscilloscope. This method achieves a bunch-by-bunch and turn-by-turn bunch-length measurement uncertainty of 1 ps. In single-bunch experiments, results obtained from the time–frequency analysis method closely matched those from the streak camera. In the study of longitudinal instability, this technique effectively captured the synchronous oscillations of the bunch length and phase. During tuning of the harmonic cavity, the system successfully observed the stretching effect of the cavity on the bunch length. It accurately resolves sub-picosecond differences between bunches within a bunch train. Furthermore, the experimental

data verified a linear relationship between the bunch-length changes and phase changes within a small range.

In summary, the existing wideband high-speed oscilloscope technology meets the requirements for bunch-by-bunch and turn-by-turn bunch-length measurements. The proposed technique of time–frequency analysis using button electrodes enables precise measurements of the longitudinal center position (phase) and bunch length. This offers a measurement resolution that is suitable for most experiments with bunch lengths above 20 ps. When the longitudinal distribution of the target bunch followed a Gaussian distribution, the performance of the measurement system surpassed that of the streak camera (a phase uncertainty better than 0.2 ps, bunch-length uncertainty better than 1 ps, and dynamic range exceeding 10 ms). This technique can be integrated as an additional module in the existing 3D bunch position measurement system HOTCAP, forming a comprehensive multiparameter bunch-by-bunch measurement system that includes the position, bunch length, and charge. It can be directly applied to any high-energy electron storage ring and serves as a powerful diagnostic tool for studying the beam impedance and nonlinear beam dynamics. In the future work, we intend to port this technique to a processor and establish an online measurement system for the real-time monitoring of beam parameter variations in storage rings.

Acknowledgements We would like to express our gratitude to SSRF and HLS for providing the research platforms and dedicated machine time. Furthermore, we appreciate the valuable discussion with Professor Bo-Cheng Jiang of Chongqing University.

Author contributions All authors contributed to the study conception and design. Material preparation, data collection, and analysis were performed by Hong-Shuang Wang, Xing Yang, Yong-Bin Leng, Yi-Mei Zhou, and Ji-Gang Wang. The first draft of the manuscript was written by Hong-Shuang Wang, and all authors commented on the previous versions of the manuscript. All authors read and approved the final manuscript.

Data availability The data that support the findings of this study are openly available in Science Data Bank at <https://cstr.cn/31253.11.sciencedb.j00186.00495> and <https://doi.org/10.57760/sciencedb.j00186.00495>.

Declarations

Conflict of interest Yong-Bin Leng is an editorial board member for Nuclear Science and Techniques and was not involved in the editorial review, or the decision to publish this article. All authors declare that there is no conflict of interest.

References

1. P. Arpaia, R. Corsini, A. Gilardi et al., Enhancing particle bunch-length measurements based on radio frequency deflector by the use of focusing elements. *Sci. Rep.* **10**, 11457 (2020). <https://doi.org/10.1103/PhysRevLett.86.2971>
2. J. Seok, M. Chung, H.S. Kang et al., Use of a corrugated beam pipe as a passive deflector for bunch length measurements. *Phys. Rev. Accel. Beams* **21**, 022801 (2018). <https://doi.org/10.1103/PhysRevAccelBeams.21.022801>
3. J. Corbett, T. Mitsuhashi, Intensity interferometer to measure short bunch length at SPEAR3. In Proceedings of IPAC2017 (Copenhagen, Denmark), (2017), pp. 60–63 <https://doi.org/10.18429/JACoW-IPAC2017-MOOCB3>
4. U. Schade, P. Kuske, J. Lee et al., Cross-correlation of THz pulses from the electron storage ring BESSY II. *Condens. Matter.* **5**, 24 (2020). <https://doi.org/10.3390/condmat5020024>
5. W. Cheng, B. Bacha, A. Blednykh et al., Longitudinal bunch profile measurement at NSLS2 storage ring. In Proceedings of IBIC2015, (Melbourne, Australia), (2015), pp. 251–255
6. J. Chen, R. Yuan, Z. Chen et al., Bunch length measurement with streak camera at SSRF storage ring. In Proceedings of IBIC2013, (Oxford, UK), (2013), pp. 478–480
7. A. Fisher, A. Novokhatski, J. Turner et al., Bunch-length measurements in PEP-II. In Proceedings of PAC2005, (Knoxville, TN), (2005), pp. 1934–1936
8. N. Hiller, S. Hillenbrand, A. Hofmann et al., Observation of bunch deformation at the ANKA storage ring. In Proceedings of IPAC2010, (Kyoto, Japan), (2010), pp. 2523–2525
9. N. Hiller, A. Hofmann, E. Huttel et al., Status of bunch deformation and lengthening studies at the ANKA storage ring. In Proceedings of IPAC2010, (San Sebastián, Spain), (2010), pp. 2951–2953
10. G. Schiwietz, J. Hwang, A. Jankowiak et al., Bunch-resolved diagnostics for a future electron-storage ring. *Nucl. Instrum. Methods A* **990**, 164992 (2021). <https://doi.org/10.1016/j.nima.2020.164992>
11. J. Byrd, W. Cheng, S. DeSantis et al., Nonlinear longitudinal dynamics studies at the ALS. In Proceedings of PAC1999 (New York, NY, USA), (1999), pp. 382–386 <https://doi.org/10.1109/PAC.1999.795711>
12. U. Iriso, F. Fernández, Streak camera measurements at ALBA: bunch length and energy matching. In Proceedings of IBIC2012, (Tsukuba, Japan), (2012), pp. 458–462
13. A. Nosych, B. Bravo, U. Iriso, Energy loss measurements with streak camera at ALBA. In Proceedings of IBIC2018, (Shanghai, China), (2018), pp. 548–551 <https://doi.org/10.18429/JACoW-IBIC2018-THOB02>
14. E. Zinin, O. Meshkov, Optical dissector for longitudinal beam profile measurement. *J. Instrum.* **10**, P10024 (2015). <https://doi.org/10.1088/1748-0221/10/10/P10024>
15. D. Malyutin, A. Matveenko, M. Ries et al., The optical dissector bunch length measurements at the Metrology Light Source, in Proceedings of IBIC2017, (Grand Rapids, MI, USA), (2017), pp. 125–128 <https://doi.org/10.18429/JACoW-IBIC2017-TUIAB3>
16. G. Niehues, E. Blomley, M. Brosi et al., High repetition rate, single-shot electro-optical monitoring of longitudinal electron bunch dynamics using the linear array detector KALYPSO. In Proceedings of IPAC2018, (Vancouver, BC, Canada), (2018), pp. 2216–2218 <https://doi.org/10.18429/JACoW-IPAC2018-WEPAL026>
17. S. Funkner, E. Blomley, E. Bründermann et al., High throughput data streaming of individual longitudinal electron bunch profiles. *Phys. Rev. Accel. Beams.* **22**, 022801 (2019). <https://doi.org/10.1103/PhysRevAccelBeams.22.022801>
18. G. Niehues, E. Bründermann, M. Caselle et al., Electro-optical diagnostics at KARA and FLUTE-results and prospects. In Proceedings of IPAC2021, (Campinas, SP, Brazil), (2021), pp. 927–930 <https://doi.org/10.18429/JACoW-IPAC2021-MOPAB293>

19. T. Ieiri, Measurement of bunch length based on beam spectrum in the KEKB. In Proceedings of EPAC2000, (Vienna, Austria), (2000), pp. 1735–1737
20. R. Kuroda, S. Kashiwagi, K. Sakaue et al., Bunch length monitor using two-frequency analysis for RF gun system. *Jpn. J. Appl. Phys.* **43**, 7747 (2004). <https://doi.org/10.1143/JJAP.43.7747>
21. F. Perez, I. Birkel, E. Huttel et al., Beam size and bunch length measurements at the ANKA storage ring. In Proceedings of PAC2003, (Portland, OR, USA), (2003), pp. 3276–3278 <https://doi.org/10.1109/PAC.2003.1289886>
22. L. Duan, Y. Leng, R. Yuan et al., Injection transient study using a two-frequency bunch length measurement system at the SSRF. *Nucl. Sci. Tech.* **28**, 93 (2017). <https://doi.org/10.1007/s41365-017-0247-2>
23. Y. Zhou, Y. Leng, B. Gao et al., Bunch length measurement using multi-frequency harmonic analysis method at SSRF. In Proceedings of IPAC2019, (Melbourne, Australia), (2019), pp. 2616–2618 <https://doi.org/10.18429/JACoW-IPAC2019-WEPGW061>
24. W. Song, T. Ha, G. Hahn et al., Online measurement of bunch lengths and fill-pattern in the PLS-II storage ring using a fast photodiode. In Proceedings of IPAC2022 (2022)
25. Y. Zhou, X. Xu, Y. Leng, Precise measurement and application of synchrotron tune at storage ring. *Nucl. Tech.* **44**, 090103 (2021). <https://doi.org/10.11889/j.0253-3219.2021.hjs.44.090103>. (in Chinese)
26. N. Zhang, L. Lai, L. Duan et al., Analysis of transverse feedback effect on beam using bunch-by-bunch position data. *Nucl. Tech.* **40**, 120101 (2017). <https://doi.org/10.11889/j.0253-3219.2017.hjs.40.120101>. (in Chinese)
27. Y. Zhou, H. Chen, S. Cao et al., Bunch-by-bunch longitudinal phase monitor at SSRF. *Nucl. Sci. Tech.* **29**, 113 (2018). <https://doi.org/10.1007/s41365-018-0445-6>
28. H. Chen, J. Chen, B. Gao et al., Bunch-by-bunch beam size measurement during injection at Shanghai Synchrotron Radiation Facility. *Nucl. Sci. Tech.* **29**, 79 (2018). <https://doi.org/10.1007/s41365-018-0420-2>
29. X. Xu, Y. Leng, B. Gao et al., HOTCAP: a new software package for high-speed oscilloscopebased three-dimensional bunch charge and position measurement. *Nucl. Sci. Tech.* **32**, 131 (2021). <https://doi.org/10.1007/s41365-021-00966-z>
30. X. Xu, Y. Leng, Y. Zhou et al., Bunch-by-bunch three-dimensional position and charge measurement in a storage ring. *Phys. Rev. Accel. Beams.* **24**, 032802 (2021). <https://doi.org/10.1103/PhysRevAccelBeams.24.032802>
31. Y. Yang, Y. Leng, Y. Yan et al., Injection performance evaluation for SSRF storage ring. *Chin. Phys. C.* **39**, 097003 (2015). <https://doi.org/10.1088/1674-1137/39/9/097003>
32. Z. Chen, T. Yang, Y. Leng et al., Wakefield measurement using principal component analysis on bunch-by-bunch information during transient state of injection in a storage ring. *Phys. Rev. Accel. Beams.* **17**, 112803 (2014). <https://doi.org/10.1103/PhysRevSTAB.17.112803>
33. Y. Zhou, Z. Chen, B. Gao et al., Bunch-by-bunch phase study of the transient state during injection. *Nucl. Instrum. Meth. A* **955**, 163273 (2020). <https://doi.org/10.1016/j.nima.2019.163273>
34. X. Xu, Y. Leng, New noninvasive measurement method of optics parameters in a storage ring using bunch-by-bunch 3D beam position measurement data. *Phys. Rev. Accel. Beams.* **24**, 062802 (2021). <https://doi.org/10.1103/PhysRevAccelBeams.24.062802>
35. V. Smaluk, Impedance computations and beam-based measurements: a problem of discrepancy. *Nucl. Instrum. Meth. A* **888**, 22–30 (2018). <https://doi.org/10.1016/j.nima.2018.01.047>
36. B. Jiang, G. Liu, Z. Dai et al., Calculation of coupling impedance of the injection section for the SSRF storage ring. *Chin. Phys. C* **30**, 22–24 (2006)
37. D. Gong, J. Gao, J. Zhai et al., Cavity fundamental mode and beam interaction in CEPC main ring. *Radiat. Detect. Technol. Methods* **2**, 17 (2018). <https://doi.org/10.1007/s41605-018-0048-0>

Publisher's Note Springer Nature remains neutral with regard to jurisdictional claims in published maps and institutional affiliations.

Springer Nature or its licensor (e.g. a society or other partner) holds exclusive rights to this article under a publishing agreement with the author(s) or other rightsholder(s); author self-archiving of the accepted manuscript version of this article is solely governed by the terms of such publishing agreement and applicable law.